The Journal of Infectious Diseases

MAJOR ARTICLE

Amylin, Aβ42, and Amyloid in Varicella Zoster Virus Vasculopathy Cerebrospinal Fluid and Infected Vascular Cells

Andrew N. Bubak,[1] Cheryl Beseler,[2] Christina N. Como,[1] Christina M. Coughlan,[1] Noah R. Johnson,[1] James E. Hassell Jr,[1] Anna M. Burnet,[1] Teresa Mescher,[1] D. Scott Schmid,[3] Colin Coleman,[1] Ravi Mahalingam,[1] Randall J. Cohrs,[1,4] Timothy D. Boyd,[1] Huntington Potter,[1] Ali H. Shilleh,[5] Holger A. Russ,[5] and Maria A. Nagel,[1,6]

[1]Department of Neurology, University of Colorado School of Medicine, Aurora, Colorado, USA, [2]Department of Psychology, Colorado State University, Fort Collins, Colorado, USA, [3] Division of Viral Diseases, National Center for Immunization and Respiratory Diseases, Centers for Disease Control and Prevention, Atlanta, Georgia, USA, [4]Department of Immunology and Microbiology, University of Colorado School of Medicine, Aurora, Colorado, USA, [5]Barbara Davis Center for Diabetes, University of Colorado School of Medicine, Aurora, Colorado, USA, and [6]Department of Ophthalmology, University of Colorado School of Medicine, Aurora, Colorado, USA

Background. Varicella zoster virus (VZV) vasculopathy is characterized by persistent arterial inflammation leading to stroke. Studies show that VZV induces amyloid formation that may aggravate vasculitis. Thus, we determined if VZV central nervous system infection produces amyloid.

Methods. Aβ peptides, amylin, and amyloid were measured in cerebrospinal fluid (CSF) from 16 VZV vasculopathy subjects and 36 stroke controls. To determine if infection induced amyloid deposition, mock- and VZV-infected quiescent primary human perineurial cells (qHPNCs), present in vasculature, were analyzed for intracellular amyloidogenic transcripts/proteins and amyloid. Supernatants were assayed for amyloidogenic peptides and ability to induce amyloid formation. To determine amylin's function during infection, amylin was knocked down with small interfering RNA and viral complementary DNA (cDNA) was quantitated.

Results. Compared to controls, VZV vasculopathy CSF had increased amyloid that positively correlated with amylin and anti-VZV antibody levels; Aβ40 was reduced and Aβ42 unchanged. Intracellular amylin, Aβ42, and amyloid were seen only in VZV-infected qHPNCs. VZV-infected supernatant formed amyloid fibrils following addition of amyloidogenic peptides. Amylin knockdown decreased viral cDNA.

Conclusions. VZV infection increased levels of amyloidogenic peptides and amyloid in CSF and qHPNCs, indicating that VZV-induced amyloid deposition may contribute to persistent arterial inflammation in VZV vasculopathy. In addition, we identified a novel proviral function of amylin.

Keywords. varicella zoster virus; vasculopathy; amyloid; amylin; Aβ42; Alzheimer disease; astrocytes.

Recent studies have shown that varicella zoster virus (VZV) reactivation increases the risk of amyloid-associated diseases. Over a 5-year follow-up period, herpes zoster ophthalmicus conferred a 2.97-fold greater risk of developing dementia ($P < .001$), of which Alzheimer disease (AD) was most common [1]. Similar findings were observed if zoster occurred in any dermatome (1.11-fold greater risk; $P < .0014$), and antiviral therapy reduced the risk [2]. Zoster also conferred a 4.62-fold increased risk of developing neovascular age-related macular degeneration over 3 years ($P < .001$) [3], and a deterioration in glycemic control among diabetic subjects [4]. Recent studies support a direct contribution of VZV to the toxic amyloid burden in these 3 diseases. Specifically, VZV infection of primary human spinal astrocytes in vitro leads to increased intracellular amyloidogenic proteins (amylin and amyloid precursor protein [APP]/amyloid-beta [Aβ]) and amyloid, as well as an extracellular environment that catalyzed amyloid formation following amylin or Aβ42 addition, likely through amyloidogenic viral peptides [5]. Another study showed that, compared to nonzoster plasma, acute zoster plasma had elevated amyloid levels and also induced aggregation of Aβ42 and amylin [6]. Herein, we determined if cerebrospinal fluid (CSF) from individuals with VZV vasculopathy contained elevated levels of amyloidogenic proteins and amyloid compared to controls with stroke. We also examined if cerebrovascular cells produced an amyloidogenic environment during VZV infection similar to that seen in VZV-infected astrocytes.

Received 5 June 2020; editorial decision 5 August 2020; accepted 11 August 2020; published online August 18, 2020.

Correspondence: Maria A. Nagel, MD, Department of Neurology, University of Colorado School of Medicine, 12700 E 19th Ave, Mail Stop B182, Aurora, CO 80045 (maria.nagel@cuanschutz.edu).

The Journal of Infectious Diseases® 2021;223:1284–94

DOI: 10.1093/infdis/jiaa513

METHODS

Human Samples, Standard Protocol Approvals, Registrations, and Patient Consent

De-identified, archived CSF from stroke subjects without (VZV^-; n = 36) and with (VZV^+; n = 16) VZV vasculopathy was obtained from Dr Ravi Mahalingam (University of Colorado), who receives specimens to evaluate for VZV vasculopathy diagnosis. These samples are not considered human subjects research by the Colorado Multiple Institutional Review Board (COMIRB protocol number 18–2410) and are deemed exempt from review as defined by its policies and regulations and US Food and Drug Administration guidelines. See Table 1 for demographics, anti-VZV antibody titers, and analyte data.

Intrathecal Antibody Assay

Enzyme-linked immunosorbent assays (ELISAs) performed by the Centers for Disease Control and Prevention (CDC) National VZV Laboratory (Atlanta, Georgia) were used to determine intrathecal synthesis of anti-VZV antibodies in concurrently obtained paired serum and CSF samples. Three commercial ELISAs (Captia herpes simplex virus type 1 [HSV-1] and herpes simplex virus type 2 [HSV-2], Trinity Biotech, Jamestown, New York; and human herpesvirus 6 [Abnova, Walnut, California]) were run as specificity controls. Patients were considered positive if serum and CSF were both positive and if VZV immunoglobulin G (IgG) serum/CSF ratios were reduced compared to total IgG or albumin ratios. Approximately 200 serum samples (obtained prior to and after age-appropriate immunization) were used as true negatives and true positives and analyzed by receiver operating characteristic (ROC) analysis; performance of glycoprotein ELISA (96% sensitive, 95% specific) and fluorescent-antibody-to-membrane-antigen test (88% sensitive, 100% specific) were independently evaluated, eliminating the need to use a "gold standard" method as a comparator [7, 8]. ROC analysis determined a cutoff value of 0.191 adjusted optical density, and a slightly more conservative cutoff of 0.200 was adopted.

CSF Thioflavin-T Fluorescence Intensity Assay

Five microliters of CSF (assayed in duplicate) was added to 195 µL of nanopure water and 75 µL of 13.5 µM of thioflavin-T (Thio-T; in 50 mM glycine; MilliporeSigma, Burlington, Massachusetts) in a black 96-well plate, incubated in the dark for 10 minutes, and fluorescence intensity measured (plate reader excitation/emission = 440/490 nm).

CSF Quantification and Statistical Analysis

CSF VZV titers and concentrations of Aβ peptides (Aβ38, Aβ40, Aβ42) and amyloid were natural log-transformed to improve normality; amylin was normally distributed in the VZV^+ group. Means and standard deviations were used to summarize the continuous biomarkers separately for each group. A χ^2 test was used for categorical variables. A 1-way random-effect analysis of variance model was used to test for VZV group effect and to compute the level of variance explained by being VZV^+. VZV group was modeled as a random variable because although VZV status was considered a "treatment," it was not controlled, and only the population from which the subjects were derived, not particular subjects, was of interest in this study. The Pearson correlation coefficient assessed correlation among measures; Cronbach coefficient α for reliability measured internal consistency among Aβ peptides.

Linear regression analysis was conducted on each group's results separately; permutation *P* value was generated due to small sample sizes. The strong VZV^+ group effect led us to explore group differences using 2 classification approaches: the classification and regression tree (CART) model and ROC curves with area under the curve (AUC) calculations. CART models use recursive partitioning to split on variables to minimize misclassification of subjects. ROC curves, generated from a binomial distribution, assess each possible cutoff value of the biomarker and classify a test result as positive or negative. Sensitivity and specificity of a biomarker(s) are calculated for each cutoff point. The AUC is a measure of diagnostic performance, where higher values represent better classification. Confidence intervals (CIs) were calculated using bootstrapping with 10 000 replicates.

Using the CART-identified optimal cutoff values, we dichotomized amylin and amyloid and conducted a causal mediation analysis under the assumption that elevated amylin reflected VZV^+ status and that amylin was an early marker of amyloid production. The effect sizes were standardized logits from logistic regression models. Bootstrapped CIs and *P* values estimate indirect and direct effects.

Analysis of variance, analysis of covariance, and ROC analyses were conducted in SAS version 9.4. Linear regression with permutation-generated *P* values was performed using R (http://www.R-project.org/). The tree package was used for CART modeling, while the pROC package in R was used to graph ROC curves and obtain bootstrapped CIs and *P* values.

Cells and Virus Infection

Quiescent primary adult human perineurial cells (qHPNCs; ScienCell, Carlsbad, California) were prepared as previously described [9, 10]; these cells were isolated from the sciatic nerve of a 55-year-old man. At day 7, qHPNCs were co-cultivated with uninfected (mock-infected) or VZV-infected qHPNCs (50 plaque-forming units/cm^2; VZV Gilden clinical strain, GenBank accession number MH379685). Cells were analyzed at 3 days postinfection (DPI) at the height of a cytopathic effect. For HSV-1 infection, cell-free virus (McKrae strain; GenBank accession number MN136524.1) was added to qHPNCs at 0.01 multiplicity of infection and removed 1 hour later; cells were analyzed at 3 DPI. CDC assays used the VZV parental Oka strain (GenBank accession number AB097933).

Table 1. Patient Information and Analyte Data for Anti–Varicella Zoster Virus Antibody Titers, Amylin, Aβ Peptides, and Thioflavin-T

Patients	Age	Sex	CSF Titer (Anti-VZV IgG)	Amylin (pM)	Aβ38 (pg/mL)	Aβ40 (pg/mL)	Aβ42 (pg/mL)	Thio-T (AU)
VZV-negative controls with stroke								
C1	64	M	0.199	6.18	595.97	1950.28	95.28	387.67
C2	59	F	0.144	8	1448.48	4911.59	275.22	1671.17
C3	37	F	0.076	7.04	435.9	1110.21	39.09	NM
C4	44	M	0.0075	4.98	1831.39	5349.71	398.13	257.67
C5	66	F	0.041	3.74	1451.63	4335.91	178.18	542.17
C6	68	F	0.105	8.46	731.35	2120.36	98.94	207.17
C7	26	M	0.064	4.84	673.24	2100.46	133.24	420.17
C8	49	M	0.023	3.92	998.22	2606.64	98.94	931.67
C9	51	M	0.001	7.68	639.8	2080.94	100.74	468.67
C10	22	M	0.18	7.79	522.58	1847.46	99.89	126.67
C11	78	M	0.09	3.32	1189.16	2781.59	129.32	521.17
C12	74	M	0.031	2.16	1366.34	4166.68	268.47	684.17
C13	46	F	0.053	8.22	954.99	2841.99	146.65	378.17
C14	22	M	0.156	7.95	730.67	2397.42	100.74	352.67
C15	53	M	0.035	4.31	1011.4	3212.61	158.55	347.17
C16	69	F	0.09	3.08	1143.01	3325.35	130.67	602.67
C17	50	F	0.142	6.14	1020.09	3039.5	152.29	NM
C18	44	F	0.195	7.78	724.59	2435.08	124.9	564.17
C19	65	M	0.01	4.18	294.5	787.92	23.81	637.17
C20	19	F	0.0115	4.39	770.33	2538.79	142.29	445.67
C21	72	F	0.091	10.61	691.75	1824.28	33.34	491.67
C22	45	F	0.015	8.83	607.69	2031.7	73.63	111.67
C23	42	F	0.0045	5.01	1459.22	4987.08	268.13	901.67
C24	45	M	0.025	5.03	897.2	3072.38	175.86	1106.67
C25	77	M	0.06	9.13	1116.97	3198.6	174.48	419.17
C26	35	M	0.07	9.24	663.41	2442.31	129.08	507.67
C27	70	M	0.06	5.24	1101.85	3787.31	114.09	926.67
C28	59	F	0.007	6.11	1880.93	6026.7	451.55	454.67
C29	45	M	0.008	11.89	577.01	2115	115.26	1294.67
C30	58	M	0.09	9.67	756.65	2908.09	125.25	963.17
C31	53	F	0.07	8.73	1099.1	4492.33	257.36	708.17
C32	44	F	0.03	9.99	561.81	2134.43	103.58	54.67
C33	35	M	0.035	12.93	1524.07	5865.8	329.37	291.67
C34	72	F	0.09	11.23	851.85	3094.72	116.77	535.17
C35	62	M	0.07	12.21	499.88	1800.62	75.88	253.17
C36	59	F	0.0075	13.55	1488.71	4677.27	277.31	421.67
VZV-positive subjects with vasculopathy								
V1	53	M	4.11	12	570.61	1150.09	138.79	1808
V2	44	F	4.8155	12.25	380.01	977.47	84.92	4135
V3	55	M	0.73	12.58	602.03	1724.07	191.49	1361
V4	33	M	0.35	11.13	428.26	1055.4	99.35	1143
V5	45	M	1.048	11.33	131.52	392.68	24.82	2216
V6	54	F	0.65	11.16	1474.15	2695.44	269.29	1126.5
V7	33	M	0.297	7.857	618.03	1285.3	142.35	844.25
V8	27	F	0.819	9.433	246.42	751.55	47.91	591.25
V9	62	M	1.843	9.231	298.52	939	98.78	1037
V10	79	F	0.213	11.05	575.75	1517.54	85	649.25
V11	75	M	2.43	8.649	345.7	926.57	61.54	1831.75
V12	65	M	3.7	7.439	772.39	1809.11	220.22	1430.75
V13	78	F	3.29	9.049	922.93	2190.95	293.65	536.25
V14	60	M	1.07	7.91	429.8	1130.73	62.4	1229.25
V15	60	F	1.1375	8.431	1377.54	2211.27	406.36	2633.25
V16	48	M	5.41	NM	2219.88	3987.74	543.44	2741.25

Abbreviations: AU, artificial units; CSF, cerebrospinal fluid; F, female; IgG, immunoglobulin G; M, male; NM, not measured; VZV, varicella zoster virus.

Amylin Small Interfering RNA Knockdown

Two independent predesigned amylin Dicer-Substrate small interfering RNAs (siRNAs) and a scramble siRNA that does not target any human or VZV genes were obtained (Integrated DNA Technologies, Coralville, Iowa; assay IDs: CD.Ri.108976.13.1, CD.Ri.108976.13.2, and catalog number 51-01-14-03, respectively). All siRNAs were diluted in RNAiMax Lipofectamine per the manufacturer's instructions and transfected into qHPNCs 1 hour before VZV infection (final concentration = 10 nM). At 3 DPI, cells were harvested and viral transcripts quantitated.

RNA Extraction and Quantitative Reverse-Transcription Polymerase Chain Reaction

At 3 DPI, RNA was reverse-transcribed into complementary DNA and analyzed by reverse-transcription quantitative polymerase chain reaction (RT-qPCR) as described previously [11]. Prevalidated primers for APP (Integrated DNA Technologies; NM_201414) and amylin (Life Technologies, Carlsbad, California; Hs00169095_m1), as well as custom VZV (open reading frame 28) and glyceraldehyde-3-phosphate-dehydrogenase (GAPDH) [10] primers [5, 12], were used. Data were normalized to GAPDH and analyzed using the ΔΔCt method or ΔCt when only 1 group amplified transcripts.

Immunofluorescence Antibody Assay and Thio-T Staining Assay

At 3 DPI, cells were analyzed by immunofluorescence antibody assay (IFA) as described previously [5]. Cells were incubated with mouse anti-VZV glycoprotein B (gB; 1:250 dilution; Abcam, Cambridge, Massachusetts) or mouse anti–HSV-1 ICP0 (1:200 dilution; Virusys Corporation, Randallstown, Maryland) and either rabbit anti-Aβ42 (1:100 dilution; Abcam) or rabbit anti-amylin (1:250 dilution; Abcam) antibodies overnight, then probed with donkey anti-rabbit Alexa Fluor 647 or donkey anti-mouse Alexa Fluor 594 IgG (both at 1:500, Life Technologies), respectively. Cell nuclei were stained with 2 μg/mL 4',6-diamidino-2-phenylindole (DAPI, Vector Laboratories, Burlingame, California). Following primary and secondary antibody stains, cells were stained with Thio-T and imaged as described elsewhere [5].

Amylin and Aβ Peptide ELISA

Human CSF and tissue culture supernatants were analyzed in duplicate for human amylin levels by ELISA (MilliporeSigma). Similarly, Aβ38, Aβ40, and Aβ42 were detected and quantified using the V-Plex Plus Aβ peptide panel 1 electrochemiluminescence immunoassay (Meso Scale Discovery, Rockville, Maryland).

Transmission Electron Microscopy

Supernatant's ability to induce Aβ42 and amylin aggregation was measured as described previously [5]. In brief, conditioned supernatant from mock- or VZV-infected qHPNCs were incubated with 4 μM Aβ42 for 1 hour or 50 μM human amylin for 72 hours at 37°C prior to preparation for imaging on a FEI Tecnai G2 Biotwin transmission electron microscope at 80 kV with an AMT side-mount digital camera.

RESULTS

Quantitation of Amyloid, Aβ Peptides, and Amylin in CSF of Stroke Subjects Without and With VZV Vasculopathy

CSF from 36 VZV^- and 16 VZV^+ stroke subjects were examined for levels of amyloid by a Thio-T assay that detects β-sheets within amyloid-like fibrillar structures (prefibrillar oligomers or amyloid fibrils) and by ELISA for levels of cellular peptides (Aβ peptides and amylin) that can aggregate to form amyloid (analyte values in Table 1). Compared to VZV^- CSF, VZV^+ CSF had significantly elevated levels of amyloid ($P < .001$) and amylin ($P < .01$), significantly decreased levels of Aβ40 ($P < .001$), and no significant changes in Aβ42 (Figure 1A) or Aβ38 (data not shown). CSF volumes were insufficient to run 2 of 36 VZV^- samples and 1 of 16 VZV^+ samples for the amyloid and amylin assays, respectively (Table 1). CSF anti-VZV antibody levels showed a significant positive correlation with amyloid in the VZV^+ group ($P < .05$; slope = 328 ± 119.8; Figure 1B); no correlation between CSF anti-VZV antibody levels and amyloid was seen in the VZV^- group. No CSF was positive for anti–HSV-1 antibodies. Thus, CSF from VZV^+ subjects was associated with elevated levels of amylin and amyloid that positively correlated with the amount of anti-VZV antibodies.

To further investigate the complex relationship of amyloid formation and amylin levels during VZV infection, VZV^- and VZV^+ CSF were compared. A strong separation of data points between VZV^- (red circles; −15.43 ± 19.75, slope ± standard error [SE]) and VZV^+ (blue squares; 166.3 ± 142.1, slope ± SE) groups was observed when assessing the relationship between amylin and amyloid (Figure 1C), although the slope coefficients were not statistically significant ($P = .06$). For CSF samples that had similar concentrations of amylin in VZV^+ and VZV^- groups (between 10 and 15 pM), amylin appeared to be positively associated with increased amyloid formation during VZV infection, whereas there was no relationship between amylin and amyloid formation in the VZV^- group (Figure 1C).

In-depth statistical analysis and modeling showed that VZV status explained 56%, 53%, 30%, and 24% of the variance in total amyloid, Aβ40, amylin, and Aβ38, respectively; VZV explained no variance in Aβ42. CART, ROC, and AUC analysis validated relevant biomarkers (amyloid, amylin, and Aβ40) important in classifying VZV status (Supplementary Figure 1*A* and 1*B*). Causal mediation model showing standardized regression coefficients for amylin as an intermediate between VZV status and amyloid formation revealed that amylin is not the sole contributor to the elevated amyloid formation measured in the VZV+ group ($P < .05$; Supplementary Figure 1*C*).

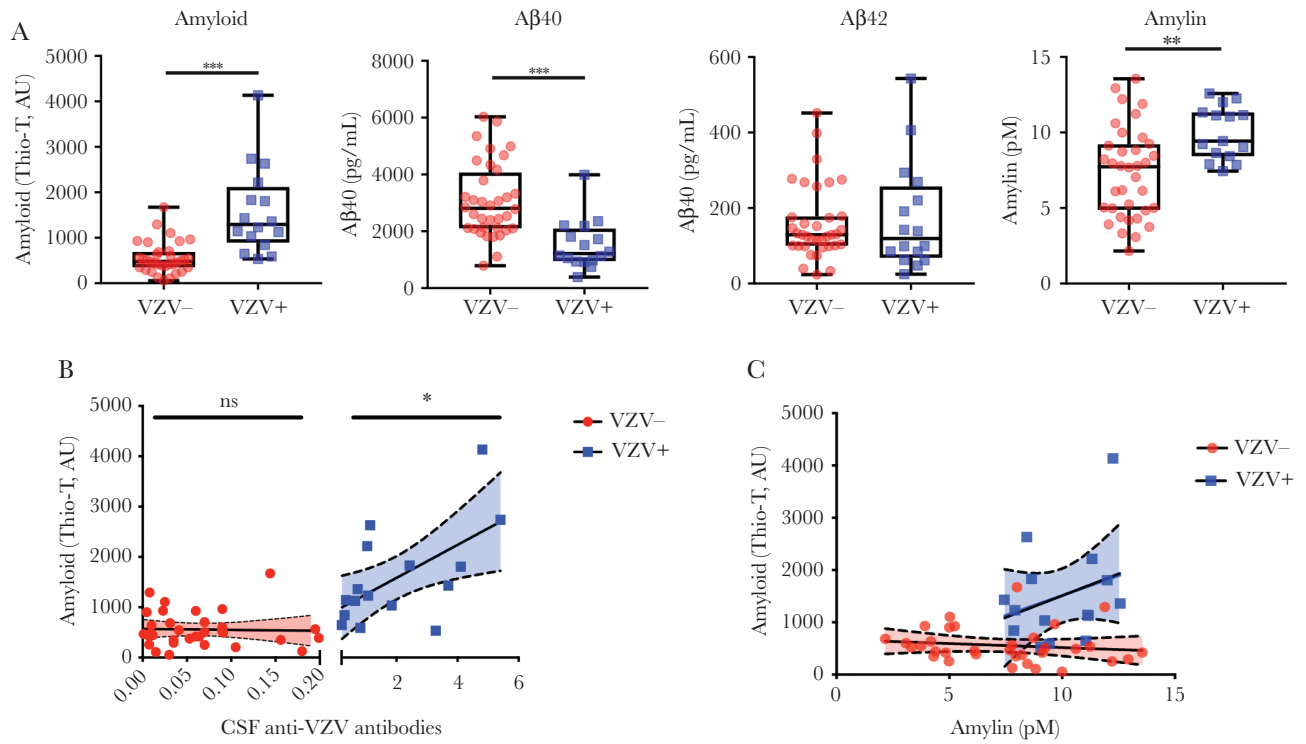

Figure 1. Amyloid, Aβ peptides, and amylin in cerebrospinal fluid (CSF) of subjects without and with varicella zoster virus (VZV) vasculopathy. *A*, Compared to CSF from 36 subjects without VZV vasculopathy (VZV^-, red circles), CSF from 16 VZV vasculopathy subjects (VZV^+, blue squares) had significantly elevated levels of amyloid, significantly decreased levels of Aβ40, insignificant changes in Aβ42, and significantly elevated levels of amylin (**$P < .01$, ***$P < .001$). *B*, Anti-VZV immunoglobulin G (IgG) antibody levels in CSF from VZV^+ subjects (blue squares) positively and significantly correlated with levels of amyloid (*$P < .05$). Conversely, anti-VZV IgG antibody levels in CSF from VZV^- subjects (red circles) did not significantly correlate with levels of amyloid ($P > .05$). *C*, Amylin is positively correlated with amyloid in VZV^+ subjects (blue squares) but no correlation was seen in VZV^- subjects (red circles). Difference in regressions approached significance ($P = .06$). Abbreviations: AU, artificial units; CSF, cerebrospinal fluid; ns, not significant; Thio-T, thioflavin T; VZV, varicella zoster virus.

VZV-Infected qHPNCs Contain Aβ42 Peptides, Amylin, and Amyloid-Like Fibrillary Structures

To determine whether in vivo alterations are a direct effect of VZV infection, in vitro studies using qHPNCs were performed. The rationale for using these cells is that during VZV reactivation from ganglionic neurons, virus travels along nerve fibers within immunoprivileged nerve bundles that are encased by perineurial cells forming the peripheral nerve-extrafascicular tissue barrier; virus must infect and disrupt perineurial cells to access surrounding tissue [10]. Moreover, VZV infection of perineurial cells has been observed in vivo in adventitia of VZV-infected giant cell arteritis temporal artery biopsies [13, 14].

We used RT-qPCR to determine if VZV infection altered transcription of amyloidogenic proteins, APP (which can be proteolytically cleaved to produce pathogenic Aβ42 peptides), and amylin. Compared to mock-infected qHPNCs at 3 DPI, APP transcripts were significantly downregulated in VZV-infected qHPNCs (mean fold change ± standard error of the mean [SEM], 0.20 ± 0.02; $P < .01$). At 3 DPI, amylin transcripts were detected in VZV-infected qHPNCs (mean ΔCt ± SEM, 13.91 ± 0.49; n = 3; Figure 2), but not in mock-infected cells. Transfecting VZV-infected qHPNCs with 2 independent siRNAs (design 1 and 2) targeted against amylin resulted in no detectable amylin transcripts, validating amylin specificity (Figure 2). To test whether the novel increase in amylin transcripts was VZV-specific or represents a nonspecific viral response, we infected qHPNCs with HSV-1 and measured amylin transcripts. Unlike VZV, HSV-1–infected qHPNCs had undetectable amylin transcripts (Figure 2).

To confirm protein expression, mock- and VZV-infected qHPNCs were analyzed by IFA. IFA showed that mock-infected qHPNCs were Thio-T-negative and did not contain VZV gB, Aβ42, or amylin (Figure 3A and 3B, respectively). In VZV-infected cultures, VZV gB-expressing qHPNCs expressed Aβ42 and amylin, and were Thio-T positive (Figure 3A and 3B, respectively). No Aβ42, amylin, or Thio-T positivity was detected in uninfected bystander cells. Thus, qHPNCs that expressed VZV gB, also expressed Aβ42 and amylin, and contained amyloid-like fibrillar structures that were absent in mock-infected and uninfected bystander cells. In HSV-1–infected cultures, qHPNCs expressing HSV-1 ICP0 antigen were positive for Aβ42 and Thio-T, which was not detected in uninfected cells (Figure 4). Unlike VZV, HSV-1–infected qHPNCs did not express amylin

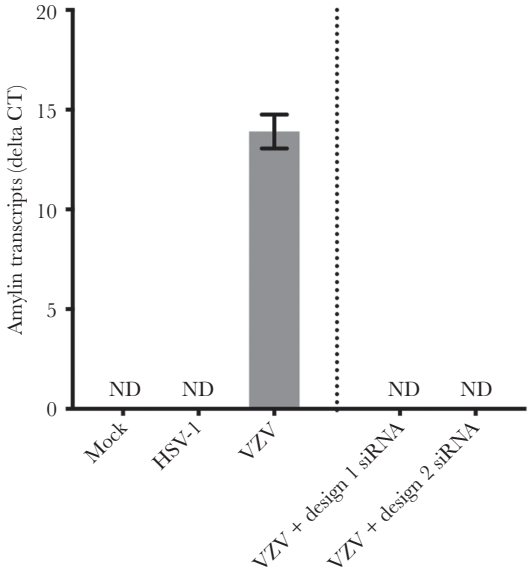

Figure 2. Varicella zoster virus (VZV), but not herpes simplex virus type 1 (HSV-1), induces amylin expression in quiescent primary adult human perineurial cells (qHPNCs). Mock- and VZV- or HSV-1–infected qHPNCs were analyzed at 3 days postinfection by reverse-transcription quantitative polymerase chain reaction for amylin transcripts. Amylin transcripts were detected in VZV-infected qHPNCs but not in mock- or HSV-1–infected qHPNCs. Amylin transcripts were not detected in VZV-infected qHPNCs that were transfected with amylin-targeted small interfering RNA (independent designs 1 and 2) 1 hour prior to infection, demonstrating specific and efficient knockdown. Bars represent mean Δ cycle threshold of amylin transcripts/glyceraldehyde-3-phosphate-dehydrogenase ± standard error of the mean. Abbreviations: Ct, cycle threshold; HSV-1, herpes simplex virus type 1; ND, not detected; siRNA, small interfering RNA; VZV, varicella zoster virus.

consistent with the undetectable amylin transcripts (Figure 2), again suggesting that the increase in amylin is a VZV-specific response.

Amylin Knockdown Decreases VZV Transcripts

To test whether VZV-induced amylin expression represents a proviral or antiviral response, qHPNCs were transfected with 1 of 2 independent siRNAs targeting amylin (design 1 or design 2) or with a scrambled siRNA (negative control) and infected with VZV 1 hour later. Knockdown of amylin expression by design 1 or 2 resulted in significant reductions in VZV transcripts when compared to scrambled siRNA transfection (Figure 5; mean fold change ± SEM, 0.4 ± 0.13 and 0.07 ± 0.02, respectively; $P < .001$). Amylin transcripts were absent in VZV-infected qHPNCs pretreated with amylin-targeted siRNA design 1 or 2, indicating knockdown of VZV-induced amylin expression (Figure 2).

Conditioned Supernatants From VZV-Infected qHPNCs Creates an Extracellular Amyloidogenic Environment

Supernatant from mock- and VZV-infected qHPNCs showed undetectable or no significant differences in amyloidogenic proteins (Aβ38, Aβ40, Aβ42, or amylin). Because VZV-infected astrocytes produced an amyloidogenic environment independent of these amyloidogenic proteins [5], we incubated the mock- and VZV-infected qHPNC supernatants with

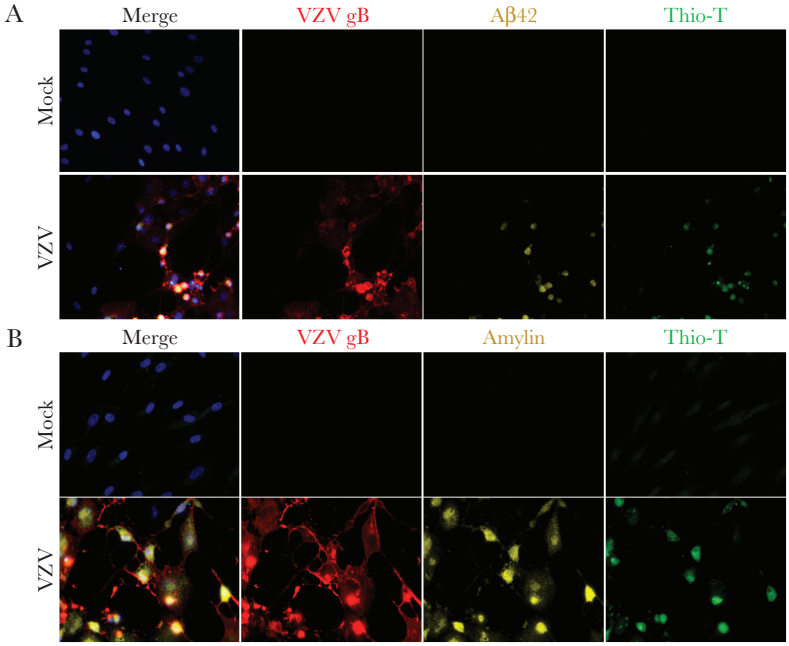

Figure 3. Varicella zoster virus (VZV)–infected quiescent primary adult human perineurial cells (qHPNCs) contain Aβ42, amylin, and amyloid-like fibrillar structures. Mock- and VZV-infected qHPNCs were analyzed at 3 days postinfection by an immunofluorescence antibody assay using antibodies against VZV glycoprotein B (gB), Aβ42, and amylin, as well as by a thioflavin-T (Thio-T) fluorescence assay that detects β-sheets in amyloid-like fibrillar structures (prefibrillar oligomers and amyloid fibrils). *A,* Mock-infected qHPNCs did not contain VZV gB or Aβ42 and were Thio-T negative. VZV-infected qHPNCs contained VZV gB (red) and Aβ42 (yellow) and were Thio-T positive (green). *B,* Similarly, mock-infected qHPNCs did not contain VZV gB or amylin and were Thio-T negative. VZV-infected qHPNCs contained VZV gB (red) and amylin (yellow) and were Thio-T positive (green). Blue corresponds to DAPI staining of cell nuclei. Original magnification ×400.

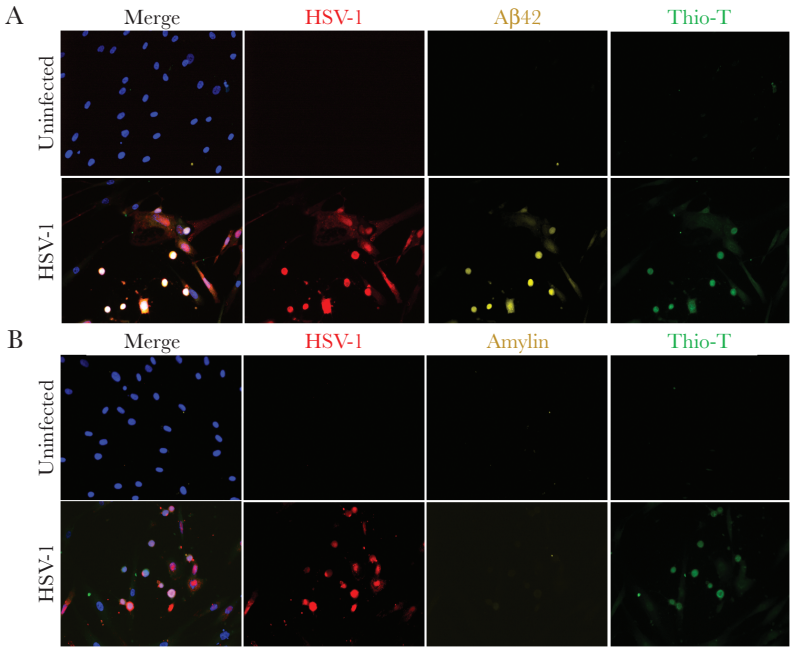

Figure 4. Herpes simplex virus type 1 (HSV-1)–infected quiescent primary adult human perineurial cells (qHPNCs) contain Aβ42 and amyloid-like fibrillar structures, but not amylin. Uninfected and HSV-1–infected qHPNCs were analyzed at 3 days postinfection by an immunofluorescence antibody assay using antibodies against HSV-1 ICP0, Aβ42, and amylin, as well as by a thioflavin-T (Thio-T) fluorescence assay that detects β-sheets in amyloid-like fibrillar structures (prefibrillar oligomers and amyloid fibrils). *A*, Uninfected qHPNCs did not contain HSV-1 ICP0 or Aβ42 and were Thio-T negative. HSV-1–infected qHPNCs contained HSV-1 ICP0 (red) and Aβ42 (yellow) and were Thio-T positive (green). *B*, Uninfected qHPNCs did not contain HSV-1 ICP0 or amylin and were Thio-T negative. HSV-1–infected qHPNCs contained HSV-1 ICP0 (red) and were Thio-T positive (green); unlike VZV-infected cells, HSV-1–infected cells did not contain amylin. Blue corresponds to DAPI staining of cell nuclei. Original magnification ×400.

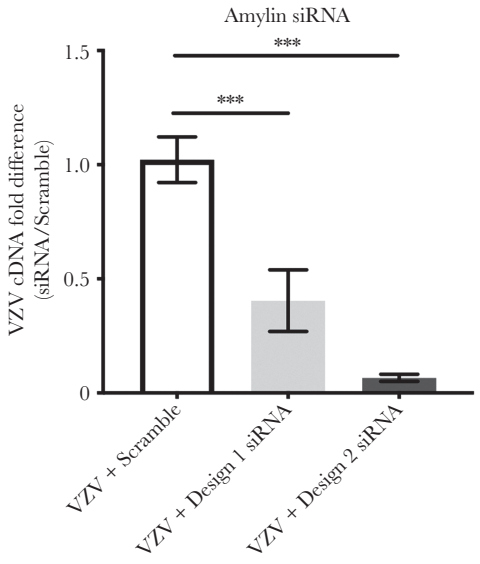

Figure 5. Varicella zoster virus (VZV)–induced amylin has a proviral function in quiescent primary adult human perineurial cells (qHPNCs). The qHPNCs were transfected with a scrambled small interfering RNA (siRNA) or 2 designs of siRNA targeting amylin 1 hour prior to VZV infection. At 3 days postinfection, compared to VZV-infected qHPNCs transfected with scrambled siRNA (n = 5), amylin-targeted siRNA design 1 (n = 3) and design 2 (n = 9) significantly reduced VZV transcripts (mean fold change ± standard error of the mean [SEM], 0.4 ± 0.13 and 0.07 ± 0.02, respectively). ***$P < .001$. Bars represent mean fold change ± SEM.

physiologically relevant concentrations of exogenous Aβ42 or amylin peptides (4 μM or 50 μM, respectively). Transmission electron microscopy revealed low levels of fibril formation in mock-infected qHPNC supernatant incubated with Aβ42 and amylin (Figure 6A and 6B, respectively, red arrows). In contrast, VZV-infected qHPNC supernatant showed elongated amyloid fibrils when Aβ42 or amylin peptides were added (Figure 6A and 6B, respectively, red arrows). Thus, VZV-infected qHPNC supernatant produced an amyloidogenic extracellular environment via increased amyloid-promoting factor(s) and/or decreased amyloid-inhibitory factor(s).

DISCUSSION

Herein, we showed that compared to CSF from stroke subjects without VZV vasculopathy, CSF from VZV vasculopathy subjects contained significantly higher levels of amylin and amyloid that positively correlated with anti-VZV antibody levels. Further statistical analysis indicated that VZV vasculopathy CSF contained factors that promote amyloid formation. Production of amylin, amyloid, and an amyloidogenic extracellular environment was shown to be a direct effect of VZV infection in qHPNCs, consistent with our previous studies in primary human spinal astrocytes [5]. In addition, the CNS amyloidogenic environment during VZV vasculopathy recapitulates the amyloidogenic environment seen in plasma during

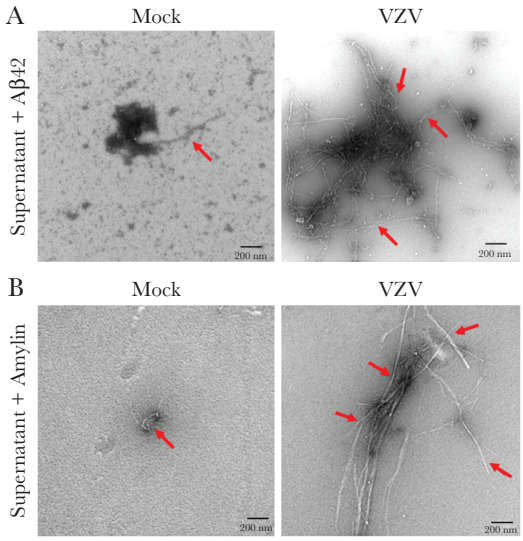

Figure 6. Conditioned supernatant from varicella zoster virus (VZV)–infected quiescent primary adult human perineurial cells (qHPNCs) creates an amyloid-promoting extracellular environment. At 3 days postinfection, supernatant from mock- and VZV-infected qHPNCs were incubated with 4 μM Aβ42 for 1 hour or 50 μM amylin for 72 hours, then visualized by transmission electron microscopy. *A,* Following incubation with Aβ42, mock-infected qHPNC supernatant had minimal amyloid fibrils, whereas VZV-conditioned supernatant developed multiple elongated amyloid fibrils. *B,* Similarly, after incubation with amylin, mock-infected qHPNC supernatant had minimal amyloid fibrils (red arrows), whereas VZV-conditioned supernatant induced the formation of elongated amyloid fibrils. Scale bar: 200 nm.

peripheral VZV infection [6]. These findings have intriguing implications in VZV vasculopathy pathogenesis and amyloid-associated diseases.

The presence of amyloid in VZV vasculopathy CSF and intracellularly in VZV-infected cells may explain, in part, the persistent inflammation in VZV-infected arteries and provides a potential link to cerebral amyloid angiopathy (CAA). VZV vasculopathy, presenting as ischemic/hemorrhagic stroke or aneurysm, occurs following VZV reactivation from trigeminal or autonomic ganglia that innervates adventitia of cerebral arteries. Virus travels along nerve fibers to infect perineurial cells and adventitial fibroblasts, then spreads inward within the arterial wall [14]. A prominent feature of VZV vasculopathy is extensive arterial infiltration of immune cells (predominantly T cells and macrophages) that release soluble factors contributing to pathological vascular remodeling [15]. Vasculitis has been attributed to VZV-induced proinflammatory cytokine release, downregulation of programmed death ligand-1 that prevents resolution of inflammation, and downregulation of major histocompatibility complex I that inhibits effective immune clearance of virus [16]. The release of intracellular amyloid and amyloidogenic cellular peptides from dying cells, as well as release of amyloidogenic viral peptides derived from VZV gB [5], in combination with detrimental environmental and host factors (ie, age-associated decrease in amyloid-degrading factors, decreased glymphatic clearance), may further contribute to persistent vascular inflammation because insoluble amyloid aggregates can chronically activate immune cells [17–20]. Furthermore, the presence of amyloid and Aβ42 in VZV-infected vascular cells raises the possibility that a subset of inflammatory cerebral amyloid angiopathy (iCAA) [21, 22] is due to VZV vasculopathy. Transient neurological symptoms and cognitive decline are present in both VZV vasculopathy [23, 24] and iCAA [25, 26]; hemorrhage and multinucleated giant cells are present in affected vessels of VZV vasculopathy [27] and iCAA [28]; and amyloid and Aβ42 are found in cerebrovascular cells in both diseases [29]. Additional support for a relationship between VZV vasculopathy and CAA comes from findings that Aβ40 is the predominant amyloidogenic peptide found in CAA [30, 31], and that CSF Aβ40 is decreased in Dutch-type hereditary CAA [32]; similarly, we also found significantly decreased Aβ40 in VZV vasculopathy (Figure 2A). The association between VZV vasculopathy and CAA is further strengthened by a recent case of CAA coexisting with VZV vasculopathy, VZV meningitis, and zoster rash [33], indicating the need to further investigate the link between these 2 diseases.

The findings that VZV induces Aβ42 expression and amyloid deposition is consistent with previous reports that HSV-1 induces Aβ42 and amyloid deposition [34–36]. Taken together with increased HSV-1 detected in brains of AD individuals, a role for HSV-1 in contributing to AD pathogenesis has been speculated (reviewed in [37]). However, in our case, our clinical samples were from individuals without AD and cognitive function was not measured; thus, we remain cautious in our interpretation of the role VZV has in AD.

Other remarkable findings include the induction of amylin by VZV in CSF and perineurial cells (similar to astrocytes in a previous study [5]), and the identification of a novel proviral function of amylin. Historically, amylin was identified as a peptide hormone that was co-secreted with insulin from pancreatic β cells in response to food intake, slowing gastric emptying and crossing the blood-brain barrier to promote satiety. Subsequently, amylin was found to aggregate into amyloid fibrils in the pancreas of >90% of subjects with diabetes mellitus (DM), forming oligomers and amyloid plaques that are cytotoxic and proinflammatory, similar to Aβ in AD brains [38, 39]. Recently, amylin has been found as independent plaques or mixed with Aβ plaques in brains of AD subjects [29], as well as in CSF of AD subjects [40]. The contribution of VZV-specific CNS amylin expression, as well as Aβ42 induction, in the context of AD pathogenesis remains to be determined, but points to VZV CNS infection as a potential accelerator of AD.

The induction of amylin appears to be VZV-specific given the lack of amylin transcripts and protein in HSV-1–infected qHPNCs. In addition, the knockdown of amylin by siRNA resulted in less VZV cDNA, indicating that amylin has a proviral function. This surprising observation differs from prior studies reporting that amylin has antimicrobial functions against

bacteria [41–43]. The mechanism(s) by which amylin potentiates VZV infection remains to be determined, yet the proviral effect of amylin may explain why individuals with DM, characterized by elevated amylin levels in pancreas and serum, are up to 30% more likely to develop zoster compared to nondiabetic controls [4, 44, 45]. Because insulin-producing pancreatic β cells are major producers of amylin, they may be more sensitive to VZV infection and associated cell death, potentially explaining the decline of glycemic control seen with zoster and the selective death of β cells in DM.

While Aβ42 was seen in VZV-infected cells, it was not elevated in VZV vasculopathy CSF; this may be because VZV-induced Aβ42 was not released as a peptide into the CSF but aggregated into amyloid or remains within the vascular wall. The production of Aβ42 in vitro likely represents an increase in APP cleavage because no increases in APP transcripts were seen, recapitulating what was found with HSV-1 infection of neuronal and glial cells in vitro [34]. The finding that VZV-infected qHPNCs produced an amyloidogenic extracellular environment is consistent with our previous studies using human spinal astrocytes [5]. Although the exact mechanisms facilitating this increased aggregation are unknown, VZV peptide fragments acting as aggregation catalysts are likely contributors [5].

CONCLUSIONS

Increased levels of amyloidogenic cellular proteins and amyloid were seen in CSF from subjects with VZV vasculopathy and intracellularly within VZV-infected qHPNCs. Importantly, VZV vasculopathy CSF and conditioned supernatant from VZV-infected qHPNCs contained factors that promoted aggregation of amyloidogenic peptides. Overall, VZV-induced amyloid aggregation could represent an important mediator in the persistent arterial inflammation seen in VZV vasculopathy.

Supplementary Data

Supplementary materials are available at *The Journal of Infectious Diseases* online. Consisting of data provided by the authors to benefit the reader, the posted materials are not copyedited and are the sole responsibility of the authors, so questions or comments should be addressed to the corresponding author.

Notes

Disclaimer. The findings and conclusions in this report are those of the authors and do not necessarily represent the official position of the Centers for Disease Control and Prevention.

Financial support. This work was supported in part by grants from the National Institutes of Health (grant numbers P01 AG032958 to M. A. N., R. M., and R. J. C.; R01 NS094758 to M. A. N.; R01 NS093716 to R. J. C., M. A. N., and A. N. B.; and R01 NS082228 to R. J. C.).

Potential conflicts of interest. All authors: No reported conflicts of interest.

All authors have submitted the ICMJE Form for Disclosure of Potential Conflicts of Interest. Conflicts that the editors consider relevant to the content of the manuscript have been disclosed.

References

1. Tsai MC, Cheng WL, Sheu JJ, et al. Increased risk of dementia following herpes zoster ophthalmicus. PLoS One **2017**; 12:e0188490.
2. Chen VC, Wu SI, Huang KY, et al. Herpes zoster and dementia: a nationwide population-based cohort study. J Clin Psychiatry **2018**; 79:16m11312.
3. Ho JD, Lin HC, Kao LT. Increased risk of neovascular age-related macular degeneration in patients with herpes zoster ophthalmicus: a retrospective cohort study. Acta Ophthalmol **2019**; 97:e321–2.
4. Munoz-Quiles C, López-Lacort M, Ampudia-Blasco FJ, Diez-Domingo J. Risk and impact of herpes zoster on patients with diabetes: a population-based study, 2009–2014. Hum Vaccin Immunother **2017**; 13:2606–11.
5. Bubak AN, Como CN, Coughlan CM, et al. Varicella-zoster virus infection of primary human spinal astrocytes produces intracellular amylin, amyloid-β, and an amyloidogenic extracellular environment. J Infect Dis **2020**; 221:1088–97.
6. Bubak AN, Beseler C, Como CN, et al. Acute zoster plasma contains elevated amyloid, correlating with Aβ42 and amylin levels, and is amyloidogenic. J Neurovirol **2020**; 26:422–8.
7. Gershon A, Steinberg S, Greenberg S, Taber L. Varicella-zoster-associated encephalitis: detection of specific antibody in cerebrospinal fluid. J Clin Microbiol **1980**; 12:764–7.
8. Wiese-Posselt M, Siedler A, Mankertz A, et al. Varicella-zoster virus seroprevalence in children and adolescents in the pre-varicella vaccine era, Germany. BMC Infect Dis **2017**; 17:356.
9. Jones D, Blackmon A, Neff CP, et al. Varicella-zoster virus downregulates programmed death ligand 1 and major histocompatibility complex class i in human brain vascular adventitial fibroblasts, perineurial cells, and lung fibroblasts. J Virol **2016**; 90:10527–34.
10. Blackmon AM, Como CN, Bubak AN, Mescher T, Jones D, Nagel MA. Varicella zoster virus alters expression of cell adhesion proteins in human perineurial cells via interleukin 6. J Infect Dis **2019**; 220:1453–61.
11. Bubak AN, Como CN, Blackmon AM, et al. Varicella zoster virus induces nuclear translocation of the neurokinin-1

receptor, promoting lamellipodia formation and viral spread in spinal astrocytes. J Infect Dis **2018**; 218:1324–35.
12. Cohrs RJ, Gilden DH. Prevalence and abundance of latently transcribed varicella-zoster virus genes in human ganglia. J Virol **2007**; 81:2950–6.
13. Gilden D, White T, Khmeleva N, et al. Prevalence and distribution of VZV in temporal arteries of patients with giant cell arteritis. Neurology **2015**; 84:1948–55.
14. Nagel MA, White T, Khmeleva N, et al. Analysis of varicella-zoster virus in temporal arteries biopsy positive and negative for giant cell arteritis. JAMA Neurol **2015**; 72:1281–7.
15. Nagel MA, Traktinskiy I, Stenmark KR, Frid MG, Choe A, Gilden D. Varicella-zoster virus vasculopathy: immune characteristics of virus-infected arteries. Neurology **2013**; 80:62–8.
16. Nagel MA, Bubak AN. Varicella zoster virus vasculopathy. J Infect Dis **2018**; 218:107–12.
17. Sondag CM, Dhawan G, Combs CK. Beta amyloid oligomers and fibrils stimulate differential activation of primary microglia. J Neuroinflammation **2009**; 6:1.
18. Morkuniene R, Zvirbliene A, Dalgediene I, et al. Antibodies bound to Aβ oligomers potentiate the neurotoxicity of Aβ by activating microglia. J Neurochem **2013**; 126:604–15.
19. Dalgėdienė I, Lučiūnaitė A, Žvirblienė A. Activation of macrophages by oligomeric proteins of different size and origin. Mediators Inflamm **2018**; 2018:7501985.
20. Morikawa S, Kaneko N, Okumura C, et al. IAPP/amylin deposition, which is correlated with expressions of ASC and IL-1β in β-cells of Langerhans' islets, directly initiates NLRP3 inflammasome activation. Int J Immunopathol Pharmacol **2018**; 32:2058738418788749.
21. Eng JA, Frosch MP, Choi K, Rebeck GW, Greenberg SM. Clinical manifestations of cerebral amyloid angiopathy-related inflammation. Ann Neurol **2004**; 55:250–6.
22. Kinnecom C, Lev MH, Wendell L, et al. Course of cerebral amyloid angiopathy-related inflammation. Neurology **2007**; 68:1411–6.
23. Silver B, Nagel MA, Mahalingam R, Cohrs R, Schmid DS, Gilden D. Varicella zoster virus vasculopathy: a treatable form of rapidly progressive multi-infarct dementia after 2 years' duration. J Neurol Sci **2012**; 323:245–7.
24. Dennis LM, Badger K, Mizoguchi R. Herpes zoster cerebral vasculopathy in a case of cognitive decline. Biomed J Sci Tech Res **2019**; 20:14751–3.
25. Greenberg SM, Rapalino O, Frosch MP. Case records of the Massachusetts General Hospital. Case 22-2010. An 87-year-old woman with dementia and a seizure. N Engl J Med **2010**; 363:373–81.
26. Chung KK, Anderson NE, Hutchinson D, Synek B, Barber PA. Cerebral amyloid angiopathy related inflammation: three case reports and a review. J Neurol Neurosurg Psychiatry **2011**; 82:20–6.
27. Gilden DH, Kleinschmidt-DeMasters BK, Wellish M, Hedley-Whyte ET, Rentier B, Mahalingam R. Varicella zoster virus, a cause of waxing and waning vasculitis. the New England Journal of Medicine case 5-1995 revisited. Neurology **1996**; 47:1441–6.
28. Streichenberger N, Girard-Madoux P, Verejan I, Pialat J, Vital C, Kopp N. Giant cell angiitis of the central nervous system with amyloid angiopathy. A case report and review of the literature. Clin Exp Pathol **1999**; 47:311–7.
29. Jackson K, Barisone GA, Diaz E, Jin LW, DeCarli C, Despa F. Amylin deposition in the brain: a second amyloid in Alzheimer disease? Ann Neurol **2013**; 74:517–26.
30. Joachim CL, Duffy LK, Morris JH, Selkoe DJ. Protein chemical and immunocytochemical studies of meningovascular beta-amyloid protein in Alzheimer's disease and normal aging. Brain Res **1988**; 474:100–11.
31. Prelli F, Castaño E, Glenner GG, Frangione B. Differences between vascular and plaque core amyloid in Alzheimer's disease. J Neurochem **1988**; 51:648–51.
32. Schultz AP, Kloet RW, Sohrabi HR, et al; Dominantly Inherited Alzheimer Network. Amyloid imaging of Dutch-type hereditary cerebral amyloid angiopathy carriers. Ann Neurol **2019**; 86:616–25.
33. Takeshita J, Nomura E, Takemaru M, Himeno T, Shimoe Y, Kuriyama M. Rapidly deteriorated lobar intracerebral hemorrhages: possible association of varicella zoster virus-vasculopathy [in Japanese]. Rinsho Shinkeigaku **2018**; 58:245–8.
34. Wozniak MA, Itzhaki RF, Shipley SJ, Dobson CB. Herpes simplex virus infection causes cellular beta-amyloid accumulation and secretase upregulation. Neurosci Lett **2007**; 429:95–100.
35. De Chiara G, Marcocci ME, Civitelli L, et al. APP processing induced by herpes simplex virus type 1 (HSV-1) yields several APP fragments in human and rat neuronal cells. PLoS One **2010**; 5:e13989.
36. Piacentini R, Civitelli L, Ripoli C, et al. HSV1 promotes $Ca2^{+}$mediated APP phosphorylation and Aβ accumulation in rat cortical neurons. Neurobiol Aging **2011**; 32:2323.e13-26.
37. Itzhaki RF. Corroboration of a major role for herpes simplex virus type 1 in Alzheimer's disease. Front Aging Neurosci **2018**; 10:324.
38. Kahn SE, Andrikopoulos S, Verchere CB. Islet amyloid: a long-recognized but underappreciated pathological feature of type 2 diabetes. Diabetes **1999**; 48:241–53.
39. Höppener JW, Ahrén B, Lips CJ. Islet amyloid and type 2 diabetes mellitus. N Engl J Med **2000**; 343:411–9.
40. Fawver JN, Ghiwot Y, Koola C, et al. Islet amyloid polypeptide (IAPP): a second amyloid in Alzheimer's disease. Curr Alzheimer Res **2014**; 11:928–40.

41. Wang L, Liu Q, Chen JC, et al. Antimicrobial activity of human islet amyloid polypeptides: an insight into amyloid peptides' connection with antimicrobial peptides. Biol Chem **2012**; 393:641–6.
42. Wang G. Human antimicrobial peptides and proteins. Pharmaceuticals **2014**; 7:545–94.
43. Miklossy J, McGeer PL. Common mechanisms involved in Alzheimer's disease and type 2 diabetes: a key role of chronic bacterial infection and inflammation. Aging **2016**; 8:575–88.
44. Kawai K, Yawn BP. Risk factors for herpes zoster: a systematic review and meta-analysis. Mayo Clin Proc **2017**; 92:1806–21.
45. Papagianni M, Metallidis S, Tziomalos K. Herpes zoster and diabetes mellitus: a review. Diabetes Ther **2018**; 9:545–50.